Low temperature transport properties and heat capacity of single-crystal Na_8Si_{46}

J. Phys.: Condens. Matter **22** (2010) 485404 (5pp) doi:10.1088/0953-8984/22/48/485404

Low temperature transport properties and heat capacity of single-crystal Na_8Si_{46}

S Stefanoski[1], J Martin[2] and G S Nolas[1]

[1] Department of Physics, University of South Florida, Tampa, FL 33620, USA
[2] Materials Science and Engineering Laboratory, Ceramics Division, National Institute of Standards and Technology, Gaithersburg, MD 20899, USA

E-mail: gnolas@usf.edu

Received 18 August 2010, in final form 20 August 2010
Published 17 November 2010
Online at stacks.iop.org/JPhysCM/22/485404

Abstract
The low temperature thermal conductivity, resistivity, and Seebeck coefficient of single-crystal Na_8Si_{46} are investigated revealing the intrinsic low temperature transport properties of this material. Metallic conduction is observed, with a higher residual resistance ratio than any other known type I clathrate. Heat capacity together with thermal conductivity provide insight into the Na disorder inside the polyhedra formed by the Si framework. Single-crystal structural refinement and thermal property analyses reveal anisotropic disorder for Na inside the tetrakaidecahedra due to a reduction in the symmetry inside these polyhedra, unlike that for Na inside the dodecahedra.

1. Introduction

Clathrates are a class of 'open-framework' materials that have frameworks built up from group IV atoms [1–3]. Many different compositions are possible within these structure types [1, 2]. They are of fundamental interest from the perspective of both bonding and their physical properties. The possible applications range from semiconductors [4], superconductivity [5], optoelectronics [6], and thermoelectrics [7, 8]. Another interest in clathrates arises from the possibility of identifying a new type of intermediate band semiconductor for photovoltaic applications [9].

The lattice of the type I clathrate is cubic with space group $Pm\bar{3}n$, and can be represented by the general formula $X_2Y_6E_{46}$, where X and Y are interstitial atoms that are encapsulated in two different polyhedra and E represents the elements Si, Ge or Sn. It is instructive to think of the crystal structure as being constructed from two different face sharing polyhedra: two pentagonal dodecahedra (E_{20}) and six tetrakaidecahedra (E_{24}) per unit cell (figure 1). These polyhedra are thus the building blocks of the type I clathrate structure. For Na_8Si_{46} the Na atoms reside at the 2*a* and 6*d* crystallographic positions, and the Si atoms that form the framework reside at three distinct crystallographic positions, 24*k*, 6*c* and 16*i* [1, 2].

The type I clathrate Na_8Si_{46} has been known since the work of Kasper *et al* [10]. The synthesis of this composition in microcrystalline form is well known and the structural properties have been well characterized [9–24]. The transport properties of Na_8Si_{46} have not been as extensively investigated [25–27]. This is partly due to the fact that microcrystalline powders of this composition are particularly

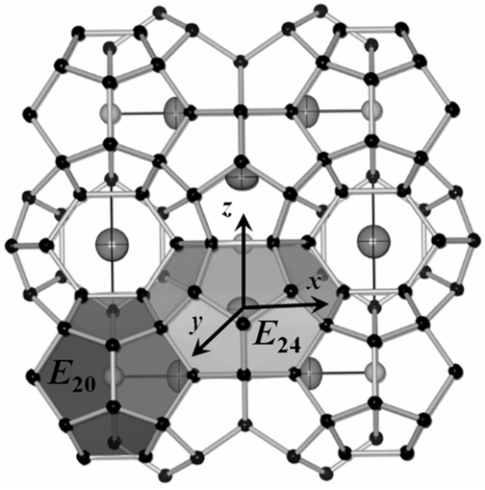

Figure 1. Crystal structure of the cubic Na_8Si_{46} type I clathrate as viewed down [100]. The Na atoms inside the dodecahedra (2*a* sites) and the tetrakaidecahedra (6*d* sites) are represented by smaller (light gray) and larger (dark gray) circles, respectively. The black circles represent Si atoms forming the framework.

difficult to densify given the low dissociation temperature [28] and the fact that silicon forms its framework [27, 28]. Moreover, an investigation into the intrinsic properties cannot be fully appreciated from polycrystalline specimens but can only be achieved by investigating specimens free of defects that may occur during densification. Here, we report on the intrinsic low temperature transport properties of single-crystal Na_8Si_{46}.

2. Experimental details

Phase-pure type I clathrate Na_8Si_{46} single-crystals were grown from a Na_4Si_4 precursor ingot using a new method: the slow controlled removal of Na via Na vapor phase intercalation of graphite. Both reactants (Na_4Si_4 and graphite) were sealed, spatially separated allowing only vapor exchange, in a steel vessel under nitrogen. The vessel was then heated at 585 °C for 8 h. Single-crystal x-ray diffraction (XRD) data, taken at 200 K, confirmed the identity and phase purity of the crystals, in the shape of truncated cubes, with a lattice parameter of 10.1973(1) Å. All Na and Si crystallographic sites showed full occupancy under refinement, confirming the stoichiometric composition Na_8Si_{46}. Isotropic atomic displacement parameters (ADPs), U_{eq} [19], from single-crystal XRD analyses indicated that U_{eq} for Na are much larger than that of the Si forming the framework, with $U_{eq} = 0.0145(3)$ Å^2 for Na inside Si_{20} and $U_{eq} = 0.0296(3)$ Å^2 for Na inside Si_{24}. These Na atoms therefore undergo localized vibrations or 'rattling'. This dynamic disorder is isotropic for the dodecahedron and anisotropic for the lower-symmetry tetrakaidecahedron. This is evident from our single-crystal structural analyses as well as our thermal property measurements, as will be described below. We note this anisotropy in the thermal ellipsoids in figure 1, obtained from our single-crystal XRD results. The coordinate system depicted within a tetrakaidecahedron in figure 1 will be used to illustrate this anisotropy. Further details of this new synthesis procedure, with detailed descriptions of the structural refinements, will be reported elsewhere [29].

The steady-state thermal conductivity, κ, Seebeck Coefficient, S, and four-probe resistivity, ρ, measurements on single-crystals of approximate dimensions 0.3 mm × 0.3 mm × 0.3 mm from 12 to 300 K were conducted in a custom radiation-shielded vacuum probe [30]. Conservative estimates of the room temperature maximum uncertainties in the measurements of κ, S and ρ are 30%, 6%, and 30%, respectively. The large uncertainties estimated for the κ and ρ measurements are due to the relatively large contacts as compared to the size of the crystals. The temperature dependent heat capacity was measured in the range 2 K $< T <$ 300 K using a commercial Quantum Design Physical Property Measurement System[3].

The data were obtained under standard thermal relaxation methods in a zero magnetic field vacuum below 1.3×10^{-5} Pa. Thermal coupling between the specimen and the specimen platform was achieved via Apiezon® N grease, where the platform is coupled to the puck via thin metal wires. Conduction through these wires is the dominant mode of thermal transfer. Prior to the specimen measurement, the specimen puck, the platform, and the Apiezon® N grease were thoroughly characterized in a separate addenda measurement. The uncertainty in the heat capacity measurements is less than 2% throughout the measured temperature range.

[3] The purpose of identifying the equipment in this article is to specify the experimental procedure. Such identification does not imply a recommendation or endorsement by the NIST.

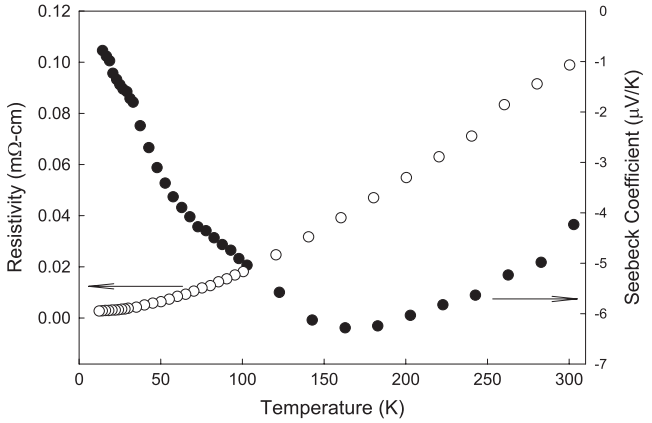

Figure 2. Temperature dependent resistivity (empty circles) and Seebeck coefficient (filled circles) for single-crystal Na_8Si_{46}.

3. Results and discussion

Figure 2 shows the temperature dependence of ρ and S for single-crystal Na_8Si_{46}. The positive $d\rho/dT$ is indicative of metallic behavior, as expected for Na_8Si_{46} due to an excess of electrons from Na. Assuming a partial charge transfer from Na to the silicon host lattice [31], with $0.694e$ per Na inside the dodecahedra and $0.783e$ per Na inside the tetrakaidecahedra where e is the elementary charge, and a unit cell volume of 1060.366 Å^3, we estimate the carrier concentration, n, to be 5.7×10^{21} cm^{-3}. In the single band approximation, assuming $\mu = (ne\rho)^{-1}$ where μ is the electron mobility, we estimate μ to be 11.2 cm^2 V^{-1} s^{-1}. This value for μ is lower than that of Cu (48 cm^2 V^{-1} s^{-1}) and comparable to that of Fe (8.2 cm^2 V^{-1} s^{-1}), calculated from the respective n and ρ for Cu and Fe [32, 33]. The inferred electron relaxation time $\tau = m/\rho ne^2 = 0.64 \times 10^{-14}$ s, where m is the free electron mass, is comparable to values for typical metals [34].

At room temperature ρ reaches a value of 0.098 mΩ cm. This value is lower than any other type I clathrate reported in the literature [25, 35–37]. A comparison between ρ measured on single-crystal Na_8Si_{46} and a consolidated polycrystalline Na_8Si_{46} specimen [25] shows that the crystal exhibits nearly two orders of magnitude lower ρ than the polycrystalline specimen. This is presumably due to the fact that the crystal is free of grain boundaries, impurities surrounding the grains, and/or defects that may occur during densification of the microcrystalline materials.

Another indicator of the quality of the single-crystal is the residual resistance ratio (RRR), defined as RRR $= R(300\text{ K})/R(T_0)$, with $T_0 = 12$ K being the lowest

temperature of our measurements. From figure 2 RRR = 36. To the best of our knowledge, this is the highest RRR of any type I clathrate reported in the literature [25, 35–37]. We note that at the lowest temperature of our measurement $d\rho/dT > 0$. This indicates that the residual resistivity has yet to be reached. S is negative in the entire temperature range and is relatively low in magnitude. This is typical for metallic compounds and is consistent with the low ρ values. The peak at ∼170 K was observed in three separate measurements on three Na_8Si_{46} crystals, and may be due to phonon-drag effects. This has also been observed in consolidated polycrystalline Na_8Si_{46} [25].

The temperature dependence of the heat capacity, C_p, for a 1.27 mg powdered specimen is shown in figure 3. We confirmed these results using three different specimen masses. The C_p values are in agreement with previous measurements from 35 to 300 K [38]. The data were fit to a straight line below 10 K according to $C_p/T = \gamma + \beta T^2$, where γ is the Sommerfield coefficient of the electronic contribution and β is the coefficient of the lattice contribution to the heat capacity [39, 40]. From this fit we obtain $\gamma = 42.5$ mJ mol^{-1} K^{-2} and $\beta = 0.5$ mJ mol^{-1} K^{-4}. From this value for γ we can estimate the density of states at the Fermi level, $N(E_F)$, using the relation [39, 41]

$$\gamma = \frac{\pi^2 k_B^2}{3} N(E_F)(1 + \lambda_{e-ph}), \tag{1}$$

where λ_{e-ph} is the electron–phonon coupling. Setting λ_{e-ph} to zero as a first approximation, the value $N(E_F) = 17.6$ states eV^{-1} per formula unit is obtained. This value is comparable to the value of 13.7 states eV^{-1} from density functional theory [9]. This high value is another indicator of the quality of the crystals [9]. Using the relation

$$\theta_D = \left(\frac{12\pi^4 R n_a}{5\beta}\right)^{1/3}, \tag{2}$$

where R is the gas constant and n_a is the number of atoms per unit cell, we estimate an effective Debye temperature, θ_D, of 542 K, similar to that of previous results [25].

The heat capacity, taking into consideration both acoustic and optic modes, has been previously described by Qiu *et al* [38]. To gain insight into the low temperature lattice dynamics, and in particular the Na 'rattle' modes, of Na_8Si_{46} we represent the total C_p as a sum of three contributions [39], the electronic contribution, $C_{el} = \gamma T$, from the electrons as heat carriers, the Debye contribution, C_D, originating from the framework, and the Einstein contribution, C_E, arising from the localized vibrations of the Na atoms inside the atomic 'cages', i.e.

$$C_p = C_{el} + C_D + C_E. \tag{3}$$

The Debye term is given by [41]

$$C_D = 9N_D R\left(\frac{T}{\theta_D}\right)^3 \int_0^{\theta_D/T} \frac{x^4 e^x}{(e^x - 1)^2}\,dx, \tag{4}$$

where N_D is the number of Debye oscillators per formula unit ($N_D = 46$ for Na_8Si_{46}), and $x = \hbar\omega/k_B T$, with ω being the phonon-angular frequency. The Einstein term is given by [42]

$$C_E = \sum_{i=1}^{N} p_i N_{Ei} R\left(\frac{\theta_{Ei}}{T}\right)^2 \frac{e^{\theta_{Ei}/T}}{(e^{\theta_{Ei}/T} - 1)^2}, \tag{5}$$

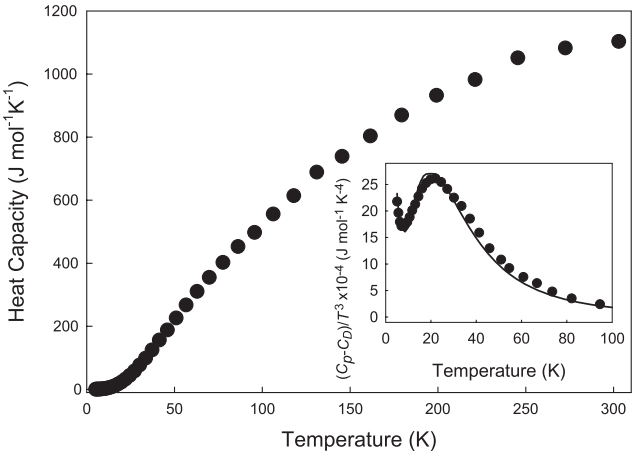

Figure 3. Heat capacity versus temperature for single-crystal Na_8Si_{46}. The inset shows $(C_p - C_D)/T^3$ plotted as a function of T. The solid line is the fit to the data according to model II, as described in the text.

Table 1. Fitting parameters for the $(C_p - C_D)/T^3$ curve according to two different models (I and II), and calculated values for the Einstein temperatures from single-crystal XRD. The free parameters in models I and II are shown in brackets. From single-crystal XRD, θ_{E1} and θ_{E2} are calculated from U_{eq} using the relation $U = k_B T/m(2\pi\nu)^2$ and $\theta_E = h\nu/k_B$, where m is the mass of Na and ν is the 'rattling' frequency, and $\theta_{E2}^{\perp}$ and $\theta_{E2}^{\parallel}$ are calculated in a similar manner using U_{22} and U_{33}, respectively.

Model (free parameters)	θ_{E1} (K)	θ_{E2} (K)	$\theta_{E2}^{\perp}$ (K)	$\theta_{E2}^{\parallel}$ (K)
I (θ_{E1}, θ_{E2})	142	81	—	—
II (θ_{E1}, $\theta_{E2}^{\perp}$, $\theta_{E2}^{\parallel}$)	162	—	163	94
XRD data	170	120	147	110

where p_i are the degrees of freedom, N_{Ei} are the number of Einstein oscillators ($N_{E1} = 2$ and $N_{E2} = 6$ for the Na atoms inside the dodecahedra and tetrakaidecahedra, respectively), and θ_{Ei} are the Einstein temperatures associated with the ith vibrational mode.

The inset to figure 3 shows $(C_p - C_D)/T^3$ versus T. The fitting parameters corresponding to two different models based on equations (3)–(5), together with Einstein temperatures estimated from our single-crystal structure refinement and analyses are listed in table 1. The free parameters for each model are also indicated in the table. The data in the inset to figure 3 are fit with a solid line according to model II in table 1. The value for γ used in equation (3) was taken from the linear fit to the low temperature C_p data. In model I the Einstein temperatures for Na inside the dodecahedra and tetrakaidecahedra are denoted by θ_{E1} and θ_{E2}, respectively. In model II the Einstein temperature for the in-plane Na vibrations (in the x–y plane in figure 1) inside the tetrakaidecahedra is denoted by $\theta_{E2}^{\parallel}$ and the Einstein temperature for the out-of-plane Na vibrations (along the z-axis in figure 1) is denoted by $\theta_{E2}^{\perp}$.

In model I we assume both θ_{E1} and θ_{E2} are isotropic. The higher value for θ_{E1} as compared to θ_{E2} (table 1) is consistent with the fact that Na has more 'room to move' in the tetrakaidecahedra compared to the dodecahedra. From our fit

$\theta_{E1} = 142$ K. This is in reasonable agreement with our single-crystal XRD results as well as that obtained from the powder XRD data from Ramachandran *et al* [22], however $\theta_{E2} = 81$ K does not agree with the single-crystal results (table 1). In addition, the center of the tetrakaidecahedron has been shown to have a lower symmetry than that of the dodecahedron in type I clathrates [43]. We therefore allow for this structural anisotropy in the tetrakaidecahedra in model II.

In model II the asymmetry of the tetrakaidecahedron requires that the Na atoms be described by a two-dimensional in-plane (the x–y plane shown in figure 1) vibrational motion characterized by $\theta_{E2}^{\parallel}$ and $p^{\parallel} \times N_{E2} = 12$, and a one-dimensional out-of-plane vibrational motion (the z-axis shown in figure 1) characterized by $\theta_{E2}^{\perp}$ and $p^{\perp} \times N_{E2} = 6$. The dodecahedron is described with an isotropic θ_{E1}. The results from fitting, $\theta_{E1} = 162$ K, $\theta_{E2}^{\perp} = 163$ K and $\theta_{E2}^{\parallel} = 94$ K, are more consistent with the single-crystal XRD results (table 1). This anisotropy within the tetrakaidecahedra in type I clathrates has been observed in ternary compositions [35, 43–45]. The pronounced peak in the inset to figure 3 centered around 25 K comes from the contribution of the localized vibrations of the Na atoms inside the Si polyhedra in Na_8Si_{46}. Theoretical investigations [12] as well as Raman scattering studies [16] on Na_8Si_{46} corroborate the peak at this temperature.

Figure 4 shows the temperature dependence of κ and the phonon mean free path, l. The κ values of single-crystal Na_8Si_{46} are higher than that of polycrystalline specimens [25], presumably due to the additional phonon scattering from the grain boundaries and higher ρ values of the polycrystalline specimen. The l values are estimated from the relation $\kappa_L = (1/3)\, lC_p\upsilon$ [41]. The lattice thermal conductivity, κ_L, is estimated using the Wiedemann–Franz relation and the resistivity values in figure 2 so that $\kappa_L = \kappa - LT/\rho$, where L is the Lorenz number with a value of 2.45×10^{-8} W Ω K^{-2}. The sound velocity, υ, is estimated from the elastic constants for Na_8Si_{46} [46]. At room temperature l is approximately 7.6 μm and increases rapidly as the temperature decreases. This value is nearly two orders of magnitude higher that reported on polycrystalline Na_8Si_{46} [25]. This is expected taking into consideration the effects of grain boundary scattering in polycrystalline Na_8Si_{46} at low temperatures. At the lowest temperature of our measurements the mean free path is comparable to the dimensions of the single-crystal specimen. This is also corroborated by our temperature dependent κ data, as shown in figure 4. Below 20 K the temperature dependence of κ approaches a T^3 dependence, as represented by the solid line in figure 4. These data indicate a 'freezing-out' of the dynamic, or 'rattle', modes of Na at low temperatures.

4. Conclusion

The intrinsic properties of single-crystal Na_8Si_{46} are measured for the first time. The resistivity and Seebeck coefficient reveal metallic behavior while the residual resistance ratio is higher than any other known type I clathrate, indicating the high quality of the Na_8Si_{46} crystal. The dynamic disorder of the Na atoms inside the polyhedra formed by the silicon framework is isotropic in the dodecahedra (Si_{20}) and anisotropic in the tetrakaidecahedra (Si_{24}). This anisotropy stems from the reduced symmetry of the tetrakaidecahedra as compared to the dodecahedra [42]. The fits to our thermal property measurements are corroborated by single-crystal structural refinements, thus revealing a more complete picture of this disorder.

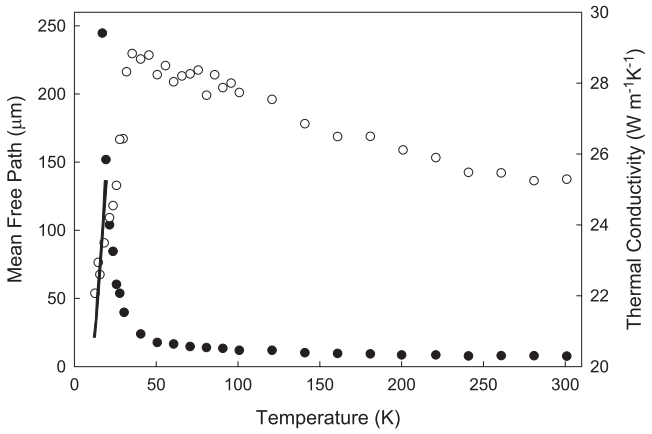

Figure 4. Mean free path (filled circles) and κ (empty circles) for single-crystal Na_8Si_{46}. The solid line shows the T^3 dependence of κ below 20 K.

Acknowledgments

SS and GSN acknowledge support from US DOE Grant no. DE-FG02-04ER46145 for the crystal growth, powder XRD and characterization, transport measurements, and data analysis. The authors acknowledge W Wong-Ng at NIST and P Zavalij at the University of Maryland for single-crystal XRD.

References

[1] Nolas G S, Slack G A and Schujman S B 2001 *Semiconductors and Semimetals* vol 69, ed T M Tritt (San Diego, CA: Academic) p 255
[2] Rogl P 2006 *Thermoelectrics Handbook: Macro to Nano* ed D M Rowe (Boca Raton, FL: CRC Press) p 32
[3] Beekman M and Nolas G S 2008 *J. Mater. Chem.* **18** 842
[4] Nolas G S, Cohn J L, Slack G A and Schujman S B 1998 *Appl. Phys. Lett.* **73** 178
[5] Herrmann R F W, Tanigaki K, Kuroshima S and Suematsu H 1998 *Chem. Phys. Lett.* **283** 29 and references therein
[6] Menon M, Richter E and Subbaswamy K 1997 *Phys. Rev.* B **56** 12290
[7] Slack G A 1997 *Mater. Res. Soc. Symp. Proc.* **478** 47
[8] Martin J, Wang H and Nolas G S 2008 *Appl. Phys. Lett.* **92** 222110
[9] Conesa J C, Tablero C and Wahnon P 2004 *J. Chem. Phys.* **120** 6142
[10] Kasper J S, Hagenmuller P, Pouchard M and Cros C 1965 *Science* **150** 1713
[11] Adams G B, O'Keefe M, Demkov A A, Sankey O F and Huang Y M 1994 *Phys. Rev.* B **46** 8048
[12] Tse J S, Li Z Q and Uehara K 2001 *Europhys. Lett.* **56** 261
[13] Kurganskii S I, Borschch N A and Pereslavtseva N S 2005 *Semiconductors* **39** 1176

[14] Demkov A A, Sankey O F and Schmidt K E 1994 *Phys. Rev.* B **50** 17001
[15] Kahn D and Lu J P 1997 *Phys. Rev.* B **56** 13898
[16] Fang S L, Grigorian L, Eklund P C, Dresselhaus G, Dresselhaus M S, Kawaji H and Yamanaka S 1998 *Phys. Rev.* B **57** 7686
[17] Gryko J, McMillan P F and Sankey O F 1996 *Phys. Rev.* B **54** 3037
[18] Ramachandran G K, McMillan P F, Diefenbacher J, Gryko J, Dong J and Sankey O F 1999 *Phys. Rev.* B **60** 12294
[19] Sales B C, Chakoumakos B C, Mandrus D and Sharp J W 1999 *J. Solid State Chem.* **146** 528
[20] He J, Klung D D, Uehara K, Preston K F, Ratcliffe C I and Tse J S 2001 *J. Phys. Chem.* B **105** 3475
[21] Gryko J, McMillan P F, Marzke R F, Dodokin A P, Demkov A A and Sankey O F 1998 *Phys. Rev.* B **57** 4172
[22] Ramachandran G K, Dong J, Diefenbacher J, Gryko J, Marzke R, Sankey O F and McMillan P 1999 *J. Solid State Chem.* **145** 716
[23] Reny E, Gravereau P, Cros C and Pouchard M 1998 *J. Mater. Chem.* **8** 2839
[24] Mélinon P, Kéghélian P, Perez A, Champagnon B, Guyot Y, Saviot L, Reny E, Cross C, Pouchard M and Dianoux A J 1999 *Phys. Rev.* B **59** 10099
[25] Nolas G S, Ward J M, Gryko J, Qiu L and White M 2001 *Phys. Rev.* B **64** 153201
[26] Tse J S, Uehara K, Rousseau R, Ker A, Ratcliffe C I, White M A and MacKay G 2000 *Phys. Rev. Lett.* **85** 114
Tse J S, Uehara K, Rousseau R, Ker A, Ratcliffe C I, White M A and MacKay G 2001 *Phys. Rev. Lett.* **86** 4980
[27] Cross C, Pouchard M and Hagenmuller P 1970 *J. Solid State Chem.* **2** 570
[28] Beekman M, Sebastian C P, Grin Yu and Nolas G S 2009 *J. Electron. Mater.* **38** 1136
[29] Stefanoski S, Beekman M, Zavalij P, Wong-Ng W and Nolas G S 2010 *Chem. Mater.* submitted
[30] Martin J, Nolas G S, Wang H and Yang J 2007 *J. Appl. Phys.* **102** 103719
[31] Volmer M, Sternemann C, Tse J S, Buslaps T, Hiraoka N, Bull C L, Gryko J, McMillan P F, Paulus M and Tolan M 2007 *Phys. Rev.* B **76** 233104
[32] Giancoli D C and Douglas C 1995 *Physics* 4th edn (Englewood Cliffs, NJ: Prentice-Hall)
[33] Anthony J W, Bideaux R A, Bladh K W and Nichols M C 2003 *Handbook of Mineralogy* (Tucson, AZ: Mineral Data Publishing)
[34] Aschroft N W and Mermin N D 1976 *Solid State Physics* (Orlando: Saunders) p 10
[35] Paschen S, Carillo-Cabrera W, Bentien A, Tran V H, Baenitz M, Grin Yu and Steglich F 2001 *Phys. Rev.* B **64** 214404
[36] Sales B C, Chakoumakos B C, Jin R, Thompson J R and Mandrus D 2001 *Phys. Rev.* B **63** 245113
[37] Avila M A, Suekuni K, Umeo K and Takabatake T 2006 *Physica* B **383** 124
[38] Qiu L, White M A, Li Z, Tse J S, Ratcliffe C I, Tulk C A, Dong J and Sankey O F 2001 *Phys. Rev.* B **64** 024303
[39] Aydemir U *et al* 2010 *Dalton Trans.* **39** 1078
[40] Singh Y, Lee Y, Nandi S, Kreyssig A, Ellern A, Das S, Nath R, Harmon B, Goldman A I and Johnston D C 2008 *Phys. Rev.* B **78** 104512
[41] Kittel C 1996 *Introduction to Solid State Physics* 7th edn (New York: Wiley)
[42] Beekman M, Schnelle W, Borrmann H, Baitinger M, Grin Yu and Nolas G S 2010 *Phys. Rev. Lett.* **104** 018301
[43] Schujman S B, Nolas G S, Young R A, Lind C, Wilkinson A P, Slack G A, Patschke R, Kanatzidis M G, Ulutagay M and Hwu S J 2000 *J. Appl. Phys.* **87** 1529
[44] Nolas G S and Kendziora C A 2000 *Phys. Rev.* B. **62** 7157
[45] Nolas G S, Weakley T J R and Cohn J L 1999 *Chem. Mater.* **11** 2470
[46] Ledbetter H M 1980 *J. Phys. D: Appl. Phys.* **13** 1879